JOURNAL OF NATURAL PRODUCTS

pubs.acs.org/jnp

Article

Genome-informed Discovery of Monchicamides A−K: Cyanobactins from the Microcoleaceae Cyanobacterium LEGE 16532

Raquel Castelo-Branco,[Δ] João P. Pereira,[Δ] Sara Freitas, Marco Preto, Ana R. Vieira, João Morais, and Pedro N. Leão*

Cite This: *J. Nat. Prod.* 2025, 88, 86−93

Read Online

ACCESS | Metrics & More | Article Recommendations | Supporting Information

ABSTRACT: Genome mining has emerged as an important tool for the discovery of natural products and is particularly effective for the swift identification of ribosomally synthesized and post-translationally modified peptides (RiPPs). Among RiPPs, cyanobactins have gained attention due to their diverse structures and bioactive properties. Here, we explored the Microcoleaceae cyanobacterium LEGE 16532 strain and identified the *mon* biosynthetic gene cluster (BGC), which was predicted to encode cyanobactin-like molecules. This led to the detection of 11 macrocyclic cyanobactins, the monchicamides, some of which feature mono- or diprenylation. One of the compounds was isolated, monchicamides I (**9**), and its planar structure was established by LC-HRESIMS/MS data as well as 1D and 2D NMR spectroscopy, confirming forward O-prenylation in Tyr. In addition, the absolute configuration of compound **9** was determined by Marfey's method and chiral-phase HPLC. The structures of the additional cyanobactins were proposed from MS/MS data analysis. The bioactivity profile of the isolated compound was also evaluated, but no cytotoxic, antimicrobial, or antiamoebic activity was observed.

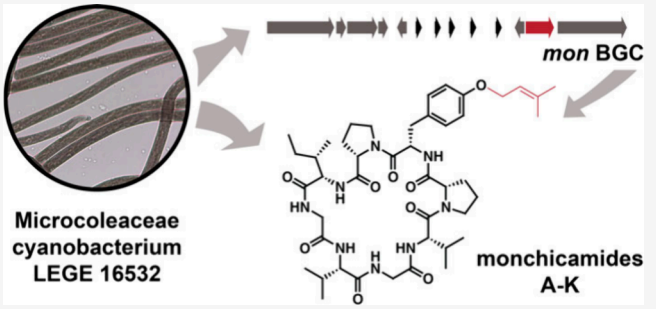

Cyanobactins are a class of ribosomally synthesized and post-translationally modified peptides (RiPPs) produced by free living or symbiotic cyanobacteria.[1,2] It is estimated that up to 30% of all cyanobacteria have the genetic capacity to produce cyanobactins.[3] These compounds have been associated with cytotoxic, multidrug reversing, antiviral, and antimalarial activities;[4] however, their natural roles remain a mystery. Cyanobactins are biosynthesized through a common pathway. Their biosynthetic gene clusters (BGCs) encode one or more precursor gene "E" which is composed of an N-terminal conserved leader sequence and a C-terminal core sequence that is found in the final natural product, flanked by recognition sequences (RSs) that facilitate the recognition by biosynthetic enzymes modifying the core peptide. The proteolytic step that removes the region preceding the core peptide (leader peptide) is mediated by the action of a subtilisin-like S8A protease "A". Subsequently, a second subtilisin-like protease "G" removes the C-terminal recognition sequence, leading to head-to-tail cyclic or linear final products.[3,5] Cyanobactins can also display heterocyclization of Ser, Thr, and Cys to oxazolines and thiazolines, which results from the action of a heterocyclase "D". Additional late-stage modifications of the peptide include oxidation of the heterocycles to oxazoles and thiazoles, as well as prenylation.[1,6] The latter modification is performed by a prenyltransferase (PTase) encoded by the "F" gene. Different PTases have been characterized including those catalyzing forward or reverse prenylation of Ser, Thr, Tyr,[7−9] C/N-prenylation of Trp,[10] bis-prenylation of Arg,[11] and a bifunctional PTase which catalyzes His/Tyr-geranylation.[12] The discovery of different classes of PTases with diverse acceptor residue specificities expands the biosynthetic toolkit for the enzymatic prenylation of peptide substrates. Prenylated peptides show increased membrane permeability and bioavailability,[13] so this modification has garnered interest as it can lead to more effective peptide therapeutics. Here, we report the discovery of 11 new cyclic cyanobactins, the monchicamides A−K (compounds **1**−**11**, Figure 2) from the Microcoleaceae cyanobacterium LEGE 16532 strain, including mono- and diprenylated, as well as nonprenylated congeners. One of the metabolites was isolated, monchicamide I (**9**), and did not exhibit cytotoxic, antimicrobial, or antiamoebic activities.

RESULTS AND DISCUSSION

Genome Mining and Detection of New Cyanobactins from Microcoleaceae Cyanobacterium LEGE 16532.

Received: September 17, 2024
Revised: December 10, 2024
Accepted: December 10, 2024
Published: December 24, 2024

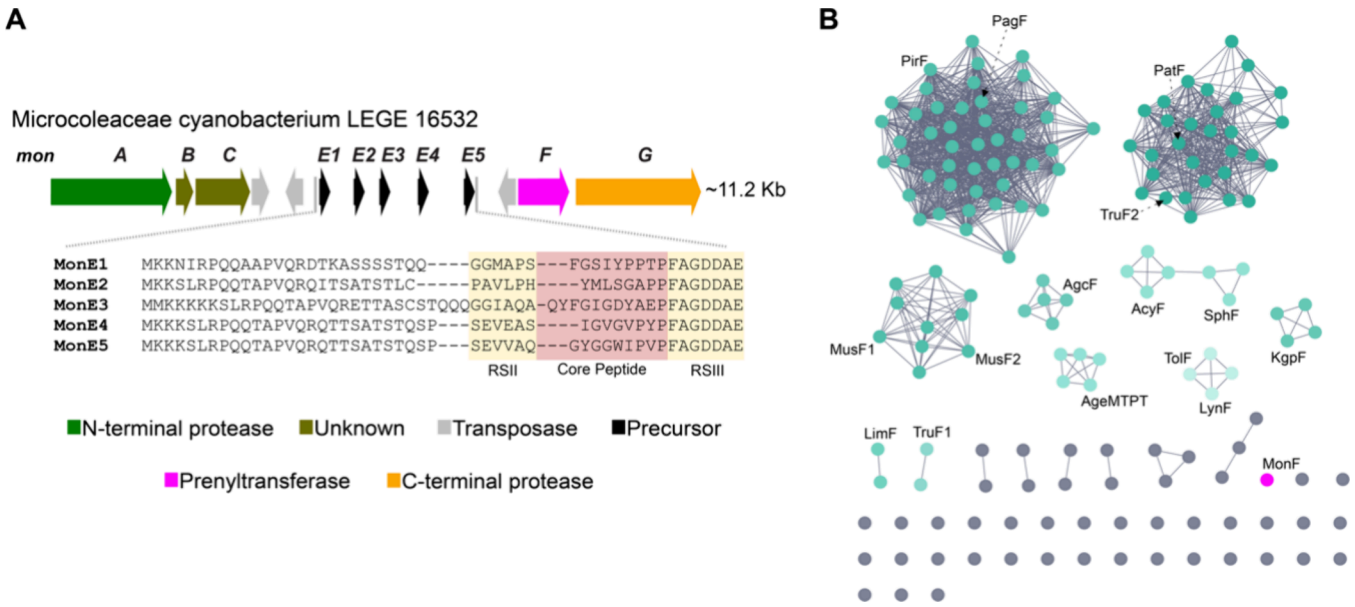

Figure 1. A) The *mon* gene cluster and sequence of precursor peptides were detected (MonE1−MonE5) with the core regions in red and RSII and RSIII highlighted in yellow. B) Sequence similarity network showing the clustering of cyanobactin PTases according to their regiospecificity using an alignment score threshold of 86.

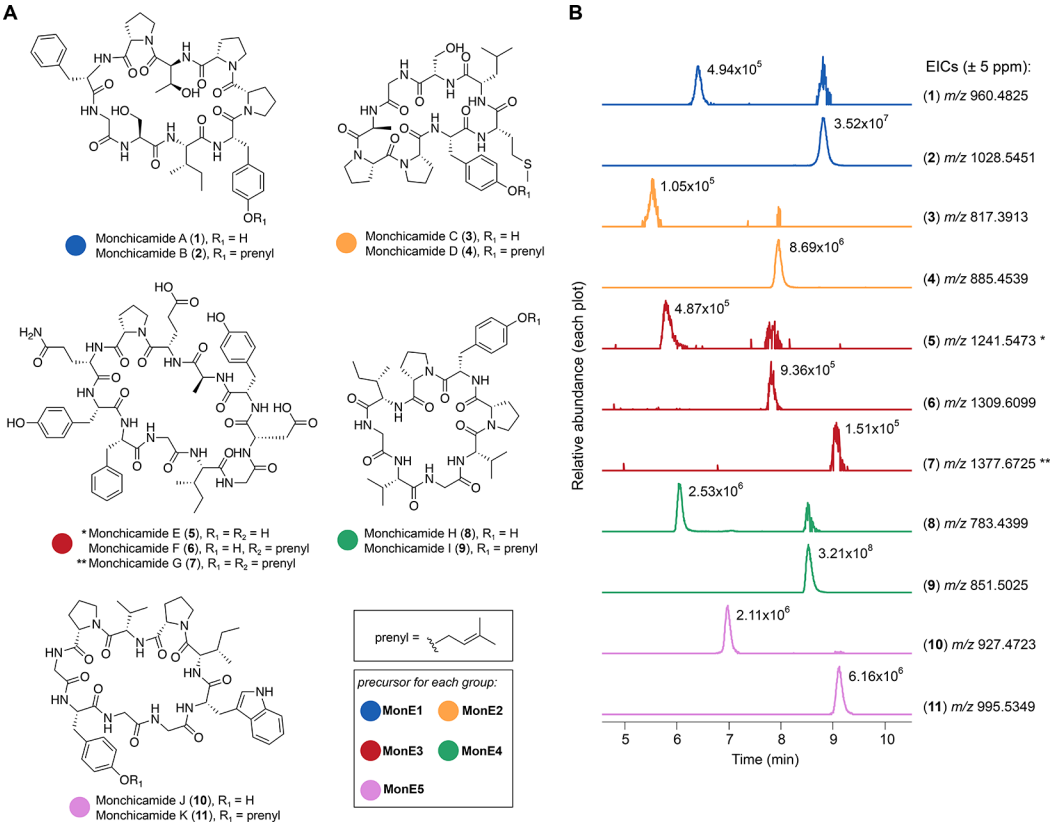

Figure 2. Discovery of monchicamides A−K. A) Structures of the herein reported cyanobactins **1**−**11**. The colors of the circles for each group correspond to those in panel B. B) LC-HRESIMS analysis of an organic extract of Microcoleaceae cyanobacterium LEGE 16532 indicates the presence of five groups of monchicamides encoded by the five precursors detected in *mon* BGC, each consisting of macrocyclic nonprenylated, mono-, and bis-prenylated variants, as illustrated by the represented Extracted Ion Chromatograms (EICs) for the $[M + H]^+$ ion of each of these compounds. * Indicates that this feature mass corresponding to the $[M + H]^+$ ion of monchicamide E (**5**) was detected in fraction F2, and ** indicates that this feature mass corresponding to the $[M + H]^+$ ion of monchicamide G (**7**) was detected in fraction F. These masses were not detected in the methanolic extract likely due to their low abundance and complexity of the extract.

Microcoleaceae cyanobacterium LEGE 16532 strain exhibited *Microcoleus*-like morphology; however, phylogenetic inferences based on the 16S rRNA gene revealed that this strain formed a separate clade from reference strains of Microcolaceae family

https://doi.org/10.1021/acs.jnatprod.4c01063
J. Nat. Prod. 2025, 88, 86−93

(Figure S1). The similarity of Microcoleaceae cyanobacterium LEGE 16532 to the reference strains is less than 96% (Table S1), suggesting that it could belong to a new genus. For this reason, a conservative approach for the identification of this strain was adopted, and it was classified at the family level. The phylogenetic distance of this strain prompted us to explore it for its natural product biosynthetic potential. Thus, the genome of Microcoleaceae cyanobacterium LEGE 16532 was sequenced and submitted to antiSMASH v7.0[14] for the identification of putative BGCs encoding natural products biosynthetic pathways. This analysis yielded a 11.2 kb cyanobactin BGC (accession number: PQ095879). We have named this BGC monchicamide (*mon*) since this strain was isolated from a water tank in the Monchique Range (Faro, Portugal). The *mon* BGC (Figure 1a, Table S2) contains the signature genes involved in cyanobactin biosynthesis.[1] In addition to genes encoding a protease (*monA*) and a macrocyclase (*monG*), the *mon* BGC includes five genes encoding different precursor peptides (*monE1*−*monE5*). Based on the recognition sequences RSII and RSIII for MonA and MonG, respectively (Figure 1a), the core peptide of each precursor was identified, ranging from 8 to 11 amino acids and presenting new core sequences such as FGSIYPPTP (MonE1), YMLSGAPP (MonE2), QYFGIGDYAEP (MonE3), IGVGVPYP (MonE4), and GYGGWIPVP (MonE5) (Figure 1a). The *mon* BGC also encodes a PTase (MonF) (50% identity, with 71% similarity to the best hit of BLASTp: *Symploca* sp. SIO1B1, NER99685.1) (Table S2). Given this distance to other PTases, a sequence similarity network (SSN) was created using MonF as a query, so as to better understand the placement of this enzyme in the sequence−function space of PTases (Figure 1b). The InterPro family of PTases (IPR031037) was included in the analysis, with an alignment score threshold of 10^{-86}. The resulting SSN revealed several clusters for which putative functions could be assigned based on the presence of characterized homologues. These included Tyr-O-prenylation (PagF and PirF),[15] terminal-N/O-prenylation (MusF1 and MusF2),[16] Arg-N-prenylation (AgcF and AutF),[11,17] Trp-N/C-prenlyation (AcyF and KgpF),[3,10] and His-C-geranylation (LimF).[12] MonF did not cluster with any other PTases, which we considered could suggest a differentiated prenylation activity. This was further supported by phylogenetic analysis (Maximum Likelihood, MF) of MonF with other characterized cyanobactin PTases (Figure S2), which showed that MonF forms a distinct clade rooted between Arg-N-PTases (AgcF and AutF) and LimF, a prenyltransferase able to perform His-C/Tyr-O-geranylation. Therefore, we decided to investigate further the products of the *mon* biosynthetic pathway.

RiPPs derive from gene-encoded precursor peptides as linear chains of amino acids produced by the ribosomes. The structural diversity observed in these peptides derives from post-translational processing of the core peptide.[18] Cyanobactin biosynthesis is well established,[19] and, based on the *monE1*−*E5* sequences, the sequence of each core with possible modifications (macrocyclization and multiple prenylations) was predicted (Table S3). An extract of freeze-dried biomass from Microcoleaceae cyanobacterium LEGE 16532 was analyzed by LC-HRESIMS, and the resulting data were searched for the exact masses of the protonated molecule of each peptide. Mass features compatible with five groups of putative macrocyclized monchicamides (corresponding to compounds **1**−**2**, **3**−**4**, **6**, **8**−**9**, and **10**−**11**) were observed (Figure 2). These consisted of nonprenylated or monoprenylated (as indicated by the diagnostic prenyl neutral loss, *m*/*z* 68.03), variants of each core peptide. At this point, it was not possible to pinpoint the prenylation site(s), or if these were forward or reverse prenylations. The exact mass of each compound was searched in the Natural Product Atlas (NAP)[20] and Dictionary of Natural Products,[21] with no hits returned.

Isolation of monchicamide I (9). To obtain structural evidence regarding prenylation type and site as well as biological activity data, we attempted the isolation of the monchicamides. Large-scale culturing (60 L) of Microcoleaceae cyanobacterium LEGE 16532 yielded 45.0 g of biomass (d.w.). This biomass was extracted by repeated percolation with MeOH, resulting in an organic extract of 4.0 g. Subsequent isolation of the cyanobactins was carried out using reversed-phase (C_{18}) vacuum liquid chromatography (VLC) with a stepwise gradient of decreasing polarity from H_2O to MeOH, resulting in seven fractions (A−G). LC-HRESIMS analysis was performed to follow the monchicamide masses throughout the isolation procedure. After the VLC step, five groups of cyanobactins (previously identified in the methanolic extraction) were found to be present. Interestingly, in fraction F (eluting with 100% MeOH), it was possible to detect an additional mass (*m*/*z* 1377.671, $[M + H]^+$) corresponding to the macrocyclic QYFGIGDYAEP core structure (encoded by the MonE3) decorated with two prenyl moieties (**7**, Figure 2). Moreover, the same fraction contained the mass feature of *m*/*z* 851.474, $[M + H]^+$ (corresponding to compound **9**), in higher relative abundance compared with the other monchicamides, motivating us to target this compound for purification. During the isolation of **9** (Figure S3), an additional mass feature corresponding to the macrocylized nonprenylated monchicamide **5** encoded by the MonE3 (*m*/*z* 1241.519, $[M + H]^+$) was detected in fraction F2 (Figure 2). Additional chromatographic steps, namely flash chromatography, semipreparative, and analytical HPLC yielded pure **9** (1.1 mg, >90% ^{1}H NMR).

Structure Elucidation of the Monchicamides. The HRESIMS data of **9** (*m*/*z* 851.47491, $[M + H]^+$) was consistent with the chemical formula $C_{44}H_{66}N_8O_9$, requiring 16 degrees of unsaturation. HRESIMS/MS fragmentation data (Figure S4) showed the sequential loss of the amino acids of the core peptide IGVGVPYP. A difference of 231.13 Da between the parent ion *m*/*z* 851.47491 $[M + H]^+$ and fragment *m*/*z* 620.375 was found to be consistent with a prenylated Tyr residue (Figure 3A and Figure S4). To confirm Tyr as the prenylated residue and to determine whether the prenylation occurred in a forward or reversed manner, we carried out 1D and 2D NMR (600 MHz, DMSO-d_6) spectroscopy for this compound. The NMR data (Table S4, Figures S5−S9) allowed to establish, in a straightforward manner, that Tyr was *O*-prenylated, owing to a key HMBC correlation between the methylene protons H_2-5 in the prenyl group and the oxygenated C-6 in the Tyr residue (Figure 3B). Furthermore, the COSY correlations for the entire spin system of the prenyl group, supported by HMBC data, were supportive of forward prenylation. The NMR data also indicated that the compound adopted several conformations in solution; still, it was possible to assign resonances supporting the precursor gene-derived amino acid sequence (Table S4, Figures S5−S9).

The absolute configuration of the amino acid residues in **9** was determined using Marfey's analysis and chiral-phase

https://doi.org/10.1021/acs.jnatprod.4c01063
J. Nat. Prod. 2025, 88, 86−93

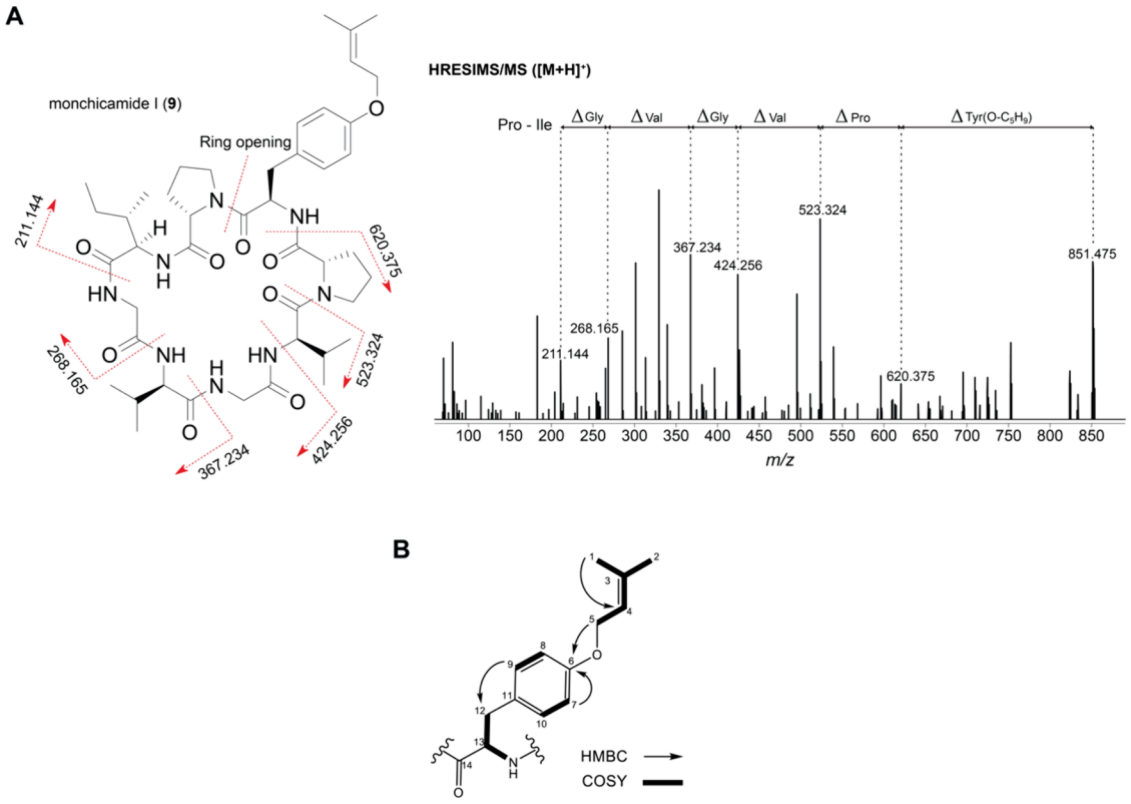

Figure 3. Structure elucidation of compound **9**. A) Annotation of key fragments observed in the HRESIMS/MS spectrum) of compound **9** (core peptide IGVGVPYP), leading to confirmation of the amino acid sequence and prenylated residue. B) Key NMR correlations supporting a forward prenylated Tyr residue.

HPLC. All chiral amino acid residues of compound **9** were found to be in the L-configuration. This is in line with the absence of epimerases in the *mon* BGC and the fact that only proteinogenic amino acids are monomers for RiPP biosynthesis.[22]

We acquired HRESIMS/MS data for the additional monchicamides (Figures S10−S19) to obtain structural information. The data for the nonprenylated representative of each of the five different groups (compounds **1**, **3**, **5**, **8**, and **10**, Figure 2) was compared to those of the monoprenylated counterparts (compounds **2**, **4**, **6**, **9**, and **11**, respectively). In all cases, it was possible to detect the fragments corresponding to the sequential loss of the amino acids that composed each core peptide. As canonical biosynthesis of these cyanobactins is to be expected, we assume that Ile (and not the isobaric Leu) is present, based on the precursor peptide sequences for MonE1, MonE3, MonE4, and MonE5. In the monoprenylated versions, the 231.13 Da mass difference for the prenylated Tyr residue was observed, confirming the prenylation position in these additional peptides. In the case of the cyanobactin encoded by the MonE3, the structure of the diprenylated **7** (m/z 1377.67139 $[M + H]^+$) was elucidated by comparison of its HRESIMS/MS data with those of the monoprenylated version, **6** (m/z 1309.60962 $[M + H]^+$). In both compounds, the fragment m/z 226.118, corresponding to a Pro-Gln fragment is observed (Figure S16). However, the fragment m/z 389.182 is observed in **6**, while in the spectrum of **7** a m/z 457.245 fragment is present. The difference (68.06 Da) is consistent with a prenylation in the additional Tyr of this core peptide. It is important to note that forward prenylation was confirmed by NMR-based structure elucidation for compound **9**, and thus we propose that it occurs in a similar fashion in the other monchicamides. Forward *O*-prenylation on a Tyr reside was previously reported in sphaerocyclamide.[8] We attribute prenylation to the activity of the PTase MonF due to its localization in the *mon* BGC and the fact that no additional PTases are found in the genome of Microcoleaceae cyanobacterium LEGE 16532. The initial hypothesis of MonF catalyzing an unusual prenylation was refuted, hence the sequence dissimilarity to other PTases did not translate in a differentiated reactivity. We propose that all amino acids present an L-configuration as confirmed for compound **9**, which is also supported by the absence of an epimerase that could be responsible for this modification as occurs in other RiPP families.[23] Overall, our findings confirmed that Microcoleaceae cyanobacterium LEGE 16532 produces 11 cyanobactins that can be attributed to the *mon* BGC.

Biological Activities. Monchicamide I (**9**) (1 mg mL^{-1}) was tested against several human cancer cell lines, namely, liver cancer cell line HepG2, colorectal adenocarcinoma cell line HCT 116, and the neuroblastoma cell line SH-SY5Y, and no cytotoxicity in the tested cell lines was observed. Additionally, compound **9** (1.0 mg mL^{-1}) was also tested against several Gram-positive and Gram-negative bacterial and fungal pathogens and showed no inhibitory activity. The effect of **9** (10 μM final concentration) on the growth and physiological state of three amoeba strains, namely *Acanthamoeba castellanii*, *Acanthamoeba polyphaga*, and *Dictyostelium discoideum*, was also tested. No loss of viability was observed compared to a positive control.

https://doi.org/10.1021/acs.jnatprod.4c01063
J. Nat. Prod. 2025, 88, 86−93

CONCLUSIONS

In this study, we report a series of new cyanobactins from Microcoleaceae cyanobacterium LEGE 16532 which include non-, mono-, and diprenylated macrocyclic octapeptides, nonapeptides, and undecapeptides. The discovery of these new cyanobactins was motivated by genome mining of the producing strain but also through the in silico study of MonF, the PTase encoded in the *mon* BGC, for which an SSN analysis suggested a potentially different catalytic function from previously characterized cyanobactin PTases. Although the monchicamides exhibit forward *O*-Tyr prenylation as previously reported for sphaerocyclamide, monchicamide G (**7**) appears to be the first cyanobactin reported with prenyl groups in two Tyr residues catalyzed by a single PTase. However, further experimentation, namely, biochemical characterization, is required to confirm if MonF indeed catalyzes both prenylations.

EXPERIMENTAL SECTION

General Experimental Procedures. Optical rotation analysis of **9** was performed using a JASCO P-2000 polarimeter with the software SpectraManager 2.14.02. The Nicolet iS5FTIR spectrometer (ThermoScientific) was used for the analysis of the infrared spectra of **9**, using the 9.8.372 software. The UV spectra of **9** was acquired on a UV-1600PC spectrometer (VWR) and using the MWAVE 1.0.20 software. 1D and 2D NMR data was acquired at the Materials Center of the University of Porto (CEMUP) using a Bruker Ascend 600 14.1 T 600 MHz instrument controlled with TopSpin 4.11 software. Compounds were analyzed in DMSO-d_6 (Sigma), and the chemical shifts (^{1}H and ^{13}C) were expressed in δ (ppm), referenced to the residual nondeuterated solvent (δ_H 2.5000, δ_C 39.520). NMR data was visualized using MestreNova 14.0.0 software. LC-HRESIMS analyses were conducted by using an UltiMate 3000 UHPLC system (Thermo Fisher), which consisted of an LPG-3400SD pump, a WPS-3000SL autosampler, and a VWD-3100 UV/vis detector. These instruments were connected to a Q Exactive Focus Hybrid Quadrupole Orbitrap mass spectrometer controlled by Q Exactive Focus Tune 2.9 and Xcalibur 4.1 software, also from Thermo Fisher Scientific. LC-HRESIMS was performed at positive mode with a scan range of m/z 200−3000, with a capillary voltage of −3.5 kV, a capillary temperature of 262.5 °C, and a sheath gas flow rate of 50 units. LC-HRESIMS/MS analysis was performed using the same parameters, and fragmentation was performed with 17,500 fwhm using higher-energy collision dissociation (HCD) with a 3.0 amu isolation window and a normalized stepped collision energy of 35 and 50. Cyanobacterial extracts and fractions were analyzed using an ACE(r) UltraCore SuperC18 column (2.5 μm, 95 Å, 75 × 2.1 mm), maintained at 40 °C. Samples were eluted at 0.35 mL min^{-1} using a linear gradient from 99.5% solution A (95% H_2O, 5% MeOH, and 0.1% formic acid v/v) and 0.5% solution B (95% isopropanol (*i*PrOH), 5% MeOH, and 0.1% formic acid, v/v) to reach 10% solution B over 0.5 min, followed by an increase to 60% solution B in 8 min and then to 90% in 1 min; these conditions were maintained for 6 min before returning to the initial conditions. Flash chromatography was conducted using a PureC-850 Flash Prep chromatography system (Buchi). HPLC separations were performed by using the Thermo Scientific UltiMate 3000 Basic system and controlled by Chromeleon software (Thermo Fisher). The chiral-phase HPLC analysis was performed in a JASCO PU-4180 HPLC pump with an MD-4010 photodiode array detector, and separations were monitored at 254 nm wavelengths. All solvents used were of MS grade for MS-based experiments, HPLC grade for HPLC analysis and purification, and ACS grade for extraction, VLC, and flash chromatography. Amino acids were purchased from Fluorochem (D-*allo*-Thr; L-*allo*-Thr; D-Ser; L-Ser; L-Val; D-Val; L-Pro; D-Pro; D-Tyr; L-Tyr; D-Thr; L-Phe; D-*allo*-Ile; L-Ile), Glenthan Life Sciences (L-Thr; D-Phe; D-Ile), and Bachem (L-*allo*-Ile). The reagent Nα-(2,4-dinitro-5-fluorophenyl)-L-alaninamide (Marfey's reagent) was purchased from Sigma-Aldrich.

Cyanobacterium Culture Conditions. The strain Microcoleaceae cyanobacterium LEGE 16532 was isolated from a water tank in Monchique Range (Faro, Portugal) and obtained from the Blue Biotechnology and Ecotoxicology Culture Collection (LEGE-CC).[24] This strain was cultured in 50 mL of Z8 medium,[25] at 25 °C, with shaking, under a 16 h/8 h light (10−30 μmol photons s^{-1} m^{-2})/dark cycle. Biomass from the stationary phase was harvested by centrifugation (5000*g*, 10 min, 4 °C, Gyrozen 2236R). For compound isolation, large-scale culturing of the strain was carried out in 20 L of polycarbonate carboys (Nalgene) for a total of 60 L, and biomass was harvested after 3−4 weeks of growth through filtration, immediately frozen, and freeze-dried, yielding 44.96 g of biomass (d.w.).

Genome Sequencing and Annotation. The strain Microcoleaceae cyanobacterium LEGE 16532 was sequenced elsewhere (MicrobesNG), using a combination of short-read Illumina and long-read Nanopore sequencing technologies. Fresh biomass, harvested after a 15-day cultivation period, was sent to the service provider. Following gDNA extraction and sequencing, raw data was submitted to a bioinformatics pipeline. Briefly, identification of the closest reference genomes for reading mapping was done using Kraken 2.[26] BWA-MEM was used to check the quality of the reads, and de novo assembly was performed using SPAdes.[27] Since the culture was not axenic, the genomic data was treated as a metagenome, and the retrieved contigs were analyzed using the binning tool MaxBin 2.0.[28] This procedure yielded a draft genome with an estimated size of 8.25 Mb distributed among 25 contigs. The genome was then submitted to antiSMASH v7.0[14] using relaxed detection settings and all features selected to detect the secondary metabolites BGCs within this strain. The *mon* BGC from Microcoleaceae cyanobacterium LEGE 16532 was manually annotated using BlastP to identify the homology and function of each open reading frames (ORFs) (Table S2).

Sequence Similarity Network. A sequence similarity network (SSN) was generated using the online Enzyme Function Initiative−Enzyme Similarity Tool (EFI-EST),[29] following a "Sequence BLAST (Basic Local Alignment Search Tool)" of MonF as input[30] and including the InterPro family of prenyltransferases (IPR031037) in the analysis. The alignment score threshold used was 10^{-86} as performed in previous works.[9,31] The generated network was visualized and analyzed using Cytoscape 3.7.1[32] to cluster PTases with different putative functions.

Phylogenetic Analyses. For the phylogenetic analysis based on the 16S rRNA gene, the sequences of Microcoleaceae cyanobacterium LEGE and representative strains of genera within Microcoleaceae were included in the analysis. The sequences were aligned using the MAFFT package in Geneious software. The resulting alignment was used for the phylogenetic analysis. An approximately maximum-likelihood tree was inferred using FastTree 2[33] (from the Geneious software package).

To generate the phylogenetic tree of prenyltransferases, characterized cyanobactin PTases sequences were downloaded from the NCBI database. The sequences were then aligned using the Clustal Omega setting in Geneious Prime. The resulting alignment was used for phylogenetic analysis. A maximum likelihood (ML) tree was built using the IQ-TREE 2 software[34] with 1000 bootstrap replicates to examine the phylogenetic relationship between the enzymes.

Small-Scale Extraction of Microcoleaceae cyanobacterium LEGE 16532 and LC-HRESIMS Analysis. For small-scale extraction, ∼30 mg of the freeze-dried biomass of the cyanobacterial strain was homogenized with liquid nitrogen and extracted using methanol (2 × 20 mL) at room temperature with shaking. The supernatant was obtained by centrifugation (5000*g*, 15 min, 4 °C, Gyrozen 2236R), and the solvent was evaporated in a rotary evaporator. The resulting extract was weighted and resuspended in MeOH LC-MS grade (1 mg mL^{-1}) and filtered through a 0.2 μm regenerated cellulose syringe filter. Five microliters (5 μL) of the extract were injected into the LC-HRESIMS system through the conditions mentioned in general methods. Based on the bioinformatics analysis, the structure of each core was predicted considering the expected post-translational

https://doi.org/10.1021/acs.jnatprod.4c01063
J. Nat. Prod. 2025, 88, 86−93

modifications (macrocyclization and prenylation), and the associated m/z values were searched in the LC-HRESIMS data of the cyanobacterial methanolic extract (Table S3).

Isolation of Monchicamide I (9). The freeze-dried biomass (44.96 g, d.w.) obtained from the large cultivation of Microcoleaceae cyanobacterium LEGE 16532 (60 L) was extracted through percolation with MeOH at room temperature and at 40 °C, affording a methanolic extract of 4.0 g. The extract was then analyzed by LC-HRESIMS to confirm the presence of the masses detected during the small-scale extraction. After this was confirmed, the extract was subjected to a vacuum liquid chromatography (VLC) using reversed-phase bulk silica gel C_{18} (C_{18}-RP; 17% C, approximately 0.7 mmol g^{-1}, part. size: 0.045−0.065 mm, Acros Organics). After silica activation, the extract was dry loaded onto the column (250 g of silica) and fractionated using a gradient of decreasing polarity: 1, 15, 30, 50, 70% MeOH (aq), 100% MeOH, and 100% CH_2Cl_2, yielding a total of seven fractions (A−G). After each separation during the isolation process, LC-HRESIMS analysis was performed to confirm in which fraction(s) the target compounds were present. Fraction F (corresponding to 100% MeOH, approximately 100 mg) was shown to contain the more abundant cyanobactins. Thus, this fraction was further separated using flash chromatography on a 40 g C_{18} silica cartridge (Silicycle). The procedure started with an initial isocratic step with 30% MeCN (aq) for 5 min, which was followed by a stepwise gradient up to 100% MeCN over 25 min. This mobile phase was maintained for 9.8 min before gradually introducing *i*PrOH, up to 50% over 5 min, a cleaning step held for 5 min. A total of 12 fractions were obtained, and the m/z value corresponding to **9** was detected in fraction F5 (13.8 mg), which was further fractionated by analytical HPLC using an Hichrom C_{18} analytical column (150 Å, 5 μm, 4.6 × 250 mm, Avantor) with a constant flow rate of 1 mL min^{-1}, at room temperature; 50 μL were injected per run. The mobile phase consisted of solvent A (H_2O), solvent B (*i*PrOH), solvent C (MeOH), and solvent D (MeCN). The program started with an isocratic step of 71.2% A/23.8% B/5% C for 5 min, followed by a linear gradient to 0.9% A/94.1% B/5% C over 25 min. After the mobile phase passes to 47.5% B/5% C/47.5% D, it is held for 5 min, before returning to the initial conditions. This separation yielded four subfractions in which compound **9** was the major component of subfraction F5B (3.52 mg). For the last purification step of **9**, subfraction F5B (3.5 mg) was separated using the same HPLC system; 50 μL were injected per run. The mobile phase consisted of solvent A (H_2O), solvent B (*i*PrOH), and solvent C (MeOH). The gradient program started with an isocratic step of 68.5% A/26.5% B/5% C for 35 min, followed by a linear gradient to 28.5% A/66.5% B/5% C over 2 min and maintained for 3 min before returning to the initial conditions. This separation led to the isolation of **9** (1.1 mg) that was subjected to NMR analysis to determine the direction of the prenylation.

*Monchicamide I (**9**).* Amorphous, white powder; $[\alpha]^{25}_{D}$ +82 (*c* 0.017, MeOH); UV (MeOH) λ_{max} (log ε) 193.5 (3.77), 209.0 (4.19), 275.0 (3.42) nm (Figure S20); IR ν_{max} 3417, 2955, 2917, 2849, 2348, 2282, 2230, 1738, 1657, 1651, 1644, 1557, 1462, 1411, 1384, 1317 cm^{-1} (Figure S21). ^1H and ^{13}C data, Table S4; LC-HRESIMS m/z 851.475 $[M + H]^+$ (calcd for $C_{44}H_{66}N_8O_9$, 850.49528).

Marfey's Derivatization Analysis. The Marfey's derivatization method was used to assign the configuration of Val and Pro residues in **9**. Prior to derivatization, compound **9** (0.14 mg) was hydrolyzed using 0.5 mL of 6 N HCl, in an oil bath at 110 °C for 24 h with continuous stirring. After 24 h, HCl was removed under a N_2 stream. L- and D- isomer standards of each amino acid were prepared at 50 mM in 50 μL of LC-MS-grade H_2O. The Marfey's reagent (1-fluoro-2,4-dinitrophenyl-5-L-alanine amide) was prepared at 1% (w/v) concentration in 100 μL of acetone.

For the hydrolysate derivatization, 100 μL of 1 M $NaHCO_3$ plus 100 μL of the Marfey's reagent solution were added to a glass vial, placed for 1 h on an oil bath at 40 °C with constant stirring. A volume of 100 μL of 1 M HCl was added to quench the solution, which was further diluted with 200 μL of MeCN (LC-MS-grade) and filtered (0.2 μm). The same procedure was applied to the amino acid standards: 50 μL of each standard were mixed with 20 μL of 1 M $NaHCO_3$ and 100 μL of the Marfey's reagent solution. After the reaction, it was quenched with 20 μL of 1 M HCl and diluted with 810 μL of MeCN (LC-MS-grade) and filtered.

After derivatization, all samples were analyzed by LC-HRESIMS, using an ACE UltraCore 2.5 SuperC18 column (75 × 2.1 mm, Avantor). Eluents were solutions A (H_2O, 0.1% v/v HCOOH) and B (MeCN, 0.1% v/v HCOOH). The separation was carried out as follows: 100% A for 1 min, then a linear gradient for 3 min to 20% B, followed by an increase to 50% B in 12 min, and after a steeper gradient to 100% B in 3 min, and held at 100% B for 2 min before returning to the initial conditions. The injection volume was 3 μL, the column oven was set to 40 °C, and the monitored wavelength was 254 nm. The acquisition was performed in positive mode. Retention times (t_R, min) for standards: L-Val 10.43, D-Val 11.91, L-Pro 8.82, and D-Pro 9.23. Retention times (t_R, min) for **9**: L-Val 10.47 and L-Pro 8.87 (Figure S25).

Chiral-Phase HPLC. This method was used to determine the configurations of the amino acid residues Ile and Tyr in compound **9**. For the acid hydrolysis, 0.07 mg of **9** were placed into 0.5 mL of 6 N HCl for 24 h at 110 °C under continuous stirring. After the reaction, HCl was removed under a N_2 stream. Amino acid standards were prepared at 0.1 mg mL^{-1} with MS-grade H_2O, and both hydrolysates were prepared at 1.0 mg mL^{-1}, also with MS-grade H_2O. Each sample was injected onto the HPLC system (10 μL), in which the stationary phase was the Chirex 3126 (d)-penicillamine column (50 × 4.6 mm, Phenomenex) and the mobile phase 1 mM $CuSO_4/H_2O$, at a 1.0 mL min^{-1} flow rate. The wavelength monitored was 254 nm. Standards for O-prenyl-L/D-Tyr were not used; rather, L/D-Tyr standards were used, assuming partial or total hydrolysis of the prenylated Tyr, as in previous absolute configuration determinations of O-prenylated amino acid residues.[8,9]

Retention times (t_R, min) for standards: L-Tyr 27.5, D-Tyr 52.0, L-Ile 18.1, L-*allo*-Ile 15.5, D-Ile 31.3, and D-*allo*-Ile 25.9. Retention times (t_R, min) for **9**: L-Tyr 27.4 and L-Ile 18.2 (Figure S27).

Bioactivity Assays. *Cytotoxicity Assays.* Human liver hepatocellular carcinoma (HepG2) and human colon carcinoma cell line HCT 116 were obtained from Sigma-Aldrich, while the neuroblastoma cell line SH-SY5Y was obtained from American Type Culture Collection (ATCC). The three human cancer cell lines were cultured at 37 °C in a humidified atmosphere of 5% CO_2, in Dulbecco's modified Eagle medium (DMEM) (Gibco, Thermo Fisher Scientific), McCoy's 5A medium (Sigma-Aldrich), and 1:1 mixture of DMEM and Ham's F12 medium (brand), respectively. All media were complemented with 10% fetal bovine serum, 1% penicillin/streptomycin, and 0.1% amphotericin. Cell viability was assessed by the MTT (3-(4,5-dimethylthiazol-2-yl)-2,5-diphenyltetrazolium bromide) assay. HepG2 and SH-SY5Y were seeded in 96-well plates at a density of 3.0×10^4 cells mL^{-1}, while HCT116 was seeded at a density of 3.3×10^4 cells mL^{-1} and incubated overnight before adding the pure compounds in triplicates at a concentration of 10 μg mL^{-1}. DMSO served as solvent (0.1%), and staurosporine (0.5%) was used as the positive control. After 48 h, 20 μL of MTT (1 mg mL^{-1}) was added to each well and incubated for 4 h. Media was removed, formazan crystals were dissolved in 100 μL of DMSO, and absorption was read at 570 nm on a microplate reader (Synergy HT, Biotek, Germany).

Antimicrobial Assays. The isolated compounds were tested against five references strains: the Gram-positive *Staphylococcus aureus* ATCC 29213 and *Bacillus subtilis* ATCC 6633, the Gram-negative *Escherichia coli* ATCC 25922 and *Salmonela typhimurium ATCC* 25241, and the yeast *Candida albicans* ATCC 10231. The antimicrobial activity was screened against all strains through the agar disc-diffusion method.[35] For the bacterial inoculation, Mueller−Hinton agar medium (Oxoid Ltd.) was used, and for fungi inoculation the Sabouraud agar medium (Oxoid Ltd.) was used. Petri dishes containing the respective media and inocula were incubated at 37 °C for 24 h, with the turbidity adjusted to the 0.5 McFarland standard (OD600 nm = 0.095−0.110). The plates were then inoculated with the adjusted culture, and 6 mm blank discs (Oxoid Ltd.) were placed on the inoculated plates and impregnated with 15 μL of the 1 mg mL^{-1} stock solution of pure

https://doi.org/10.1021/acs.jnatprod.4c01063
J. Nat. Prod. 2025, 88, 86−93

compound dissolved in DMSO. Blank discs impregnated with 15 μL of DMSO were utilized as negative controls. Following a 30 min incubation at room temperature, the plates were further incubated at 37 °C for 24 h, and the antimicrobial activity was determined by the development of inhibition halos.

Antiamoebic Assays. *Acanthamoeba castellanii*, *Acanthamoeba polyphaga* (both freshwater amoebae), and *Dictyostelium discoideum* (soil amoeba) were grown in 5 mL of PYG medium in 25 cm^2 flasks and incubated at 25 °C for 1 week. The suspension was transferred to a 75 cm^2 flask with fresh PYG medium and incubated for 2−3 additional days at 25 °C. For the experiments, each strain of amoebae was quantified by adding 10 μL of 0.4% Trypan Blue solution to 10 μL of culture, and the viable cells were determined by counting using a disposable slide hemocytometer. To study the antiamoebic effect of the pure cyanobactins against *A. castellanii*, *A. polyphaga*, and *D. discoideum*, a colorimetric assay was used by evaluating the cell viability using Alamar Blue. Briefly, 10^6 cells mL^{-1} of each strain of amoeba was seeded on a 96-well microtiter plate and incubated for 1 h at 25 °C. A final concentration of 10 μM (0.5 μL of a stock solution of 2 mM) of the pure compound was tested for each strain; DMSO (0.5 μL of DMSO 0.5%) and the detergent chlorhexidine digluconate (0.5 μL of a stock solution at 20 mM) were used as negative and positive controls, respectively, and the plate was then incubated for 24 h at 25 °C. Finally, 10 μL of the alamarBlue reagent (ThermoFisher) was added to each well to measure the cells viability. Plates were incubated for 4 h at 25 °C. The plates were read using a microplate reader (BioTek Cytation 5 Cell Imaging Multimode Reader, Agilent) with fluorescence wavelengths of excitation and emission set at 560 and 590 nm, respectively. All assays were performed in triplicate.

■ ASSOCIATED CONTENT

Data Availability Statement

HRESIMS/MS spectra for **1**−**11** are available through the MassIVE repository (massive.uscd.edu) under the identifier MSV000095446 and in GNPS Library under accessions CCMSLIB00012558649−CCMSLIB00012558659. Annotated nucleotide data of *mon* BGC have been deposited in GenBank under the accession number PQ095879. NMR data for **9** was deposited in Figshare under doi: 10.6084/m9.figshare.27026620.

Supporting Information

The Supporting Information is available free of charge at https://pubs.acs.org/doi/10.1021/acs.jnatprod.4c01063.

Phylogenetic trees of 16S rRNA gene and prenyltransferases; fractionation scheme for the isolation of **9**; HRESIMS/MS, ^1H, ^{13}C, HSQC, HMBC, and COSY spectra of **9**; HRESIMS/MS of compounds **1**−**8**, **10**, and **11**; UV−vis profile, FT-IR data, Marfey's derivatization and chiral-phase HPLC analysis of **9**; similarity matrix based on 16S rRNA gene sequences; annotation of the *mon* BGC; NMR table of **9**; and table with calculated and observed masses of monchicamides. (PDF)

■ AUTHOR INFORMATION

Corresponding Author

Pedro N. Leão − *Interdisciplinary Centre of Marine and Environmental Research (CIIMAR/CIMAR), University of Porto, 4450-208 Matosinhos, Portugal;* orcid.org/0000-0001-5064-9164; Email: pleao@ciimar.up.pt

Authors

Raquel Castelo-Branco − *Interdisciplinary Centre of Marine and Environmental Research (CIIMAR/CIMAR), University of Porto, 4450-208 Matosinhos, Portugal*

João P. Pereira − *Interdisciplinary Centre of Marine and Environmental Research (CIIMAR/CIMAR), University of Porto, 4450-208 Matosinhos, Portugal*

Sara Freitas − *Interdisciplinary Centre of Marine and Environmental Research (CIIMAR/CIMAR), University of Porto, 4450-208 Matosinhos, Portugal*

Marco Preto − *Interdisciplinary Centre of Marine and Environmental Research (CIIMAR/CIMAR), University of Porto, 4450-208 Matosinhos, Portugal*

Ana R. Vieira − *Interdisciplinary Centre of Marine and Environmental Research (CIIMAR/CIMAR), University of Porto, 4450-208 Matosinhos, Portugal*

João Morais − *Interdisciplinary Centre of Marine and Environmental Research (CIIMAR/CIMAR), University of Porto, 4450-208 Matosinhos, Portugal*

Complete contact information is available at: https://pubs.acs.org/10.1021/acs.jnatprod.4c01063

Author Contributions

[Δ]R.C.-B. and J.P.P. contributed equally.

Author Contributions

The manuscript was written through contributions of all authors. All authors have given approval to the final version of the manuscript.

Funding

This work is funded by national funds through FCT (Fundação para a Ciência e a Tecnologia), namely strategic funding grants UIDB/04423/2020, UIDP/04423/2020 and a PhD Scholarship to RCB (SFRH/BD/136367/2018), and through the European Union's Horizon 2020 Research and Innovation Programme (GA no. 952374).

Notes

The authors declare no competing financial interest.

■ ACKNOWLEDGMENTS

We thank the LEGE Culture Collection for providing the strain Microcoleaceae cyanobacterium LEGE 16532. We acknowledge the funding from Fundação para a Ciência e a Tecnologia through the scholarship SFRH/BD/136367/2018 to RCB. PNL acknowledges funding from the European Union's Horizon 2020 programme (WIDESPREAD, Grant Agreement 952374) and Fundação para a Ciência e a Tecnologia (FCT) through strategic funding grants UIDB/04423/2020 and UIDP/04423/2020.

■ REFERENCES

(1) Donia, M. S.; Ravel, J.; Schmidt, E. W. *Nat. Chem. Biol.* **2008**, *4* (6), 341−343.

(2) Martins, J.; Vasconcelos, V. *Marine Drugs* **2015**, *13* (11), 6910.

(3) Leikoski, N.; Liu, L.; Jokela, J.; Wahlsten, M.; Gugger, M.; Calteau, A.; Permi, P.; Kerfeld, C. A.; Sivonen, K.; Fewer, D. P. *Chemistry & biology* **2013**, *20* (8), 1033−1043.

(4) Sivonen, K.; Leikoski, N.; Fewer, D. P.; Jokela, J. *Appl. Microbiol. Biotechnol.* **2010**, *86* (5), 1213−1225. Donia, M. S.; Schmidt, E. W. *Chemistry & biology* **2011**, *18* (4), 508−519. Tianero, M. D.; Pierce, E.; Raghuraman, S.; Sardar, D.; McIntosh, J. A.; Heemstra, J. R.; Schonrock, Z.; Covington, B. C.; Maschek, J. A.; Cox, J. E.; et al. *Proc. Natl. Acad. Sci. U. S. A.* **2016**, *113* (7), 1772−1777.

(5) Sardar, D.; Pierce, E.; McIntosh, J. A.; Schmidt, E. W. *ACS Synth. Biol.* **2015**, *4* (2), 167−176.

(6) Gu, W.; Dong, S. H.; Sarkar, S.; Nair, S. K.; Schmidt, E. W. *Methods Enzymol* **2018**, *604*, 113−163.

(7) McIntosh, J. A.; Lin, Z.; Tianero, M. D.; Schmidt, E. W. *ACS Chem. Biol.* **2013**, *8* (5), 877−883.
(8) Martins, J.; Leikoski, N.; Wahlsten, M.; Azevedo, J.; Antunes, J.; Jokela, J.; Sivonen, K.; Vasconcelos, V.; Fewer, D. P.; Leao, P. N. *Sci. Rep* **2018**, *8* (1), No. 14537.
(9) Purushothaman, M.; Sarkar, S.; Morita, M.; Gugger, M.; Schmidt, E. W.; Morinaka, B. I. *Angewandte Chemie (International ed. in English)* **2021**, *60* (15), 8460−8465.
(10) Parajuli, A.; Kwak, D. H.; Dalponte, L.; Leikoski, N.; Galica, T.; Umeobika, U.; Trembleau, L.; Bent, A.; Sivonen, K.; Wahlsten, M.; et al. *Angewandte Chemie (International ed. in English)* **2016**, *55* (11), 3596−3599. Dalponte, L.; Parajuli, A.; Younger, E.; Mattila, A.; Jokela, J.; Wahlsten, M.; Leikoski, N.; Sivonen, K.; Jarmusch, S. A.; Houssen, W. E.; et al. *Biochemistry* **2018**, *57* (50), 6860−6867.
(11) Phan, C. S.; Matsuda, K.; Balloo, N.; Fujita, K.; Wakimoto, T.; Okino, T. *J. Am. Chem. Soc.* **2021**, *143* (27), 10083−10087.
(12) Zhang, Y.; Hamada, K.; Nguyen, D. T.; Inoue, S.; Satake, M.; Kobayashi, S.; Okada, C.; Ogata, K.; Okada, M.; Sengoku, T.; et al. *Nature Catalysis* **2022**, *5* (8), 682−693.
(13) Zheng, Y.; Cong, Y.; Schmidt, E. W.; Nair, S. K. *Accounts of chemical research* **2022**, *55* (9), 1313−1323.
(14) Blin, K.; Shaw, S.; Augustijn, H. E.; Reitz, Z. L.; Biermann, F.; Alanjary, M.; Fetter, A.; Terlouw, B. R.; Metcalf, W. W.; Helfrich, E. J. N.; et al. *Nucleic acids research* **2023**, *51*, W46.
(15) Hao, Y.; Pierce, E.; Roe, D.; Morita, M.; McIntosh, J. A.; Agarwal, V.; Cheatham, T. E., 3rd; Schmidt, E. W.; Nair, S. K. *Proc. Natl. Acad. Sci. U. S. A.* **2016**, *113* (49), 14037−14042. Morita, M.; Hao, Y.; Jokela, J. K.; Sardar, D.; Lin, Z.; Sivonen, K.; Nair, S. K.; Schmidt, E. W. *J. Am. Chem. Soc.* **2018**, *140* (19), 6044−6048.
(16) Mattila, A.; Andsten, R. M.; Jumppanen, M.; Assante, M.; Jokela, J.; Wahlsten, M.; Mikula, K. M.; Sigindere, C.; Kwak, D. H.; Gugger, M.; et al. *ACS Chem. Biol.* **2019**, *14* (12), 2683−2690.
(17) Clemente, C.; Johnson, N.; Ouyang, X.; Popin, R. V.; Dall'Angelo, S.; Wahlsten, M.; Jokela, J.; Colombano, A.; Nardone, B.; Fewer, D. P.; et al. *Chem. Commun. (Camb)* **2022**, *58* (86), 12054−12057.
(18) Do, T.; Link, A. J. *Biochemistry* **2023**, *62* (2), 201−209.
(19) Montalban-Lopez, M.; Scott, T. A.; Ramesh, S.; Rahman, I. R.; van Heel, A. J.; Viel, J. H.; Bandarian, V.; Dittmann, E.; Genilloud, O.; Goto, Y.; et al. *Natural product reports* **2021**, *38* (1), 130−239.
(20) van Santen, J. A.; Jacob, G.; Singh, A. L.; Aniebok, V.; Balunas, M. J.; Bunsko, D.; Neto, F. C.; Castano-Espriu, L.; Chang, C.; Clark, T. N.; et al. *ACS Cent Sci.* **2019**, *5* (11), 1824−1833.
(21) Dictionary of Natural Products. *CHEMnetBASE*. dnp.chemnetbase.com. (accessed 2024).
(22) Mordhorst, S.; Ruijne, F.; Vagstad, A. L.; Kuipers, O. P.; Piel, J. *RSC Chem. Biol.* **2023**, *4* (1), 7−36.
(23) Funk, M. A.; van der Donk, W. A. *Accounts of chemical research* **2017**, *50* (7), 1577−1586.
(24) Ramos, V.; Morais, J.; Castelo-Branco, R.; Pinheiro, Â.; Martins, J.; Regueiras, A.; Pereira, A. L.; Lopes, V. R.; Frazão, B.; Gomes, D.; et al. *Journal of Applied Phycology* **2018**, *30*, 1437.
(25) Kotai, J. *Oikos* **1972**, *15*, 155−165.
(26) Wood, D. E.; Salzberg, S. L. *Genome Biol.* **2014**, *15* (3), No. R46.
(27) Prjibelski, A.; Antipov, D.; Meleshko, D.; Lapidus, A.; Korobeynikov, A. *Curr. Protoc Bioinformatics* **2020**, *70* (1), No. e102.
(28) Wu, Y. W.; Simmons, B. A.; Singer, S. W. *Bioinformatics* **2016**, *32* (4), 605−607.
(29) Gerlt, J. A.; Bouvier, J. T.; Davidson, D. B.; Imker, H. J.; Sadkhin, B.; Slater, D. R.; Whalen, K. L. *Biochim. Biophys. Acta* **2015**, *1854* (8), 1019−1037.
(30) Camacho, C.; Boratyn, G. M.; Joukov, V.; Vera Alvarez, R.; Madden, T. L. *BMC Bioinformatics* **2023**, *24* (1), 117.
(31) Zhang, Y.; Goto, Y.; Suga, H. *Trends Biochem. Sci.* **2023**, *48* (4), 360−374.
(32) Shannon, P.; Markiel, A.; Ozier, O.; Baliga, N. S.; Wang, J. T.; Ramage, D.; Amin, N.; Schwikowski, B.; Ideker, T. *Genome research* **2003**, *13* (11), 2498−2504.
(33) Price, M. N.; Dehal, P. S.; Arkin, A. P. *PLoS One* **2010**, *5* (3), No. e9490.
(34) Minh, B. Q.; Schmidt, H. A.; Chernomor, O.; Schrempf, D.; Woodhams, M. D.; von Haeseler, A.; Lanfear, R. *Mol. Biol. Evol.* **2020**, *37* (5), 1530−1534.
(35) Dickert, H.; Machka, K.; Braveny, I. *Infection* **1981**, *9* (1), 18−24.

https://doi.org/10.1021/acs.jnatprod.4c01063
J. Nat. Prod. 2025, 88, 86−93